Extreme self-compression along with superbroad spectrum up-conversion of few-cycle optical solitons in the ionization regime

A. V. Kim, A. G. Litvak, V. A. Mironov, and S. A. Skobelev
Institute of Applied Physics, Russian Academy of Sciences, 46 Ulyanov st, 603950 Nizhny Novgorod, Russia and University of Nizhny Novgorod, 23 Gagarin Ave, 603950 Nizhny Novgorod, Russia
(Received 3 April 2015; published 30 September 2015)

A regime of extreme self-compression of optical solitons to single-cycle duration with further shortening along with superbroad spectrum up-shifting is revealed when the Kerr nonlinearity and ionization process are independently controlled. This results in efficient optical-pulse compression as a whole towards extremely short single-cycle pulses at essentially shorter wavelengths, which may open a new way to generate optical pulses with durations of hundreds of attoseconds in the ultraviolet domain.

DOI: 10.1103/PhysRevA.92.033856 PACS number(s): 42.65.Jx, 42.50.−p

I. INTRODUCTION

The concept of optical solitons have played an important role in the recent development of nonlinear optics. Two remarkable applications of soliton dynamics are supercontinuum generation and laser-pulse self-compression down to single-cycle duration [1–3]. Recently, the concept of conventional optical solitons was extended to few-cycle pulses for which the traditional envelope approach is not valid [4,5]. Of course, there are earlier examples in optical physics where the wave equation for the real laser field is treated in the context of solitons or extremely short pulses, but most of them deal with light propagation in two-level systems [6–8] or Raman-active [9] media.

From a practical point of view, producing tunable few-cycle pulses of high energies is still a formidable task in contemporary laser physics. Whereas in the infrared range, such pulses can be generated at particular wavelengths by conventional solid-state systems, e.g., based on Ti:sapphire or optical parametric chirped-pulse-amplification technologies. No analogous techniques are available in the optical and ultraviolet domains. Nevertheless, for high-energy pulses there are a number of nonlinearities that can be employed for pulse shortening; for instance, the relativistic nonlinearity or plasma effects (see Refs. [10–12]). Here, we pay particular attention to the ionization nonlinearity that has a strong impact on pulse propagation dynamics. The fundamental issue of this interaction follows from the fast ionization of atoms strongly modifying the index of refraction, even on a timescale less than the optical period. This leads to a number of interesting nonlinear phenomena such as ionization instabilities [13,14], frequency blueshifting [15,16], high-order harmonics, and terahertz generation [17,18]. It is also important to emphasize that the ionization nonlinearity is able by itself to ensure essential self-frequency up-shifting and pulse self-compression [19,20]. Based on these effects a new way of reaching petawatt-class pulses of few-cycle duration was recently proposed [21]. With the advent of gas-filled hollow-core photonic fibers (HC-PCF), nonlinear fiber optics where the Kerr nonlinearity together with the ionization nonlinearity can be self-consistently employed, brings new opportunities for controlling the spectrum and pulse evolution [22]. In particular, in Refs. [23–25] soliton blueshifting as well as self-compression effects are discussed based on the conventional compression scheme which allows shortening pulses even to single-cycle duration. However, the most intriguing question is the following: can we expect further shortening of a single-cycle pulse as a whole?

In this paper we show that, in media with independent control of the Kerr and ionization nonlinearities, such as a mixture of two gases with noticeably differing ionization potentials, there may occur extreme pulse compression. Detailed analysis shows that this could open a new way to generate pulses with durations of hundreds of attoseconds in the ultraviolet domain having energy efficiency up to forty percent, which is much higher than attainable with available methods. The gas with a higher potential (and a higher density) provides the Kerr nonlinearity and thus keeps the soliton as a stable structure, whereas the second ionizing gas provides frequency up-shifting. A waveguide system is proposed to be used to control the wave velocity dispersion. In this case, the soliton self-compression regime consists of two qualitatively different consecutive stages. In the first stage, the soliton pulse is compressed conventionally, when the process evolves adiabatically matching the soliton relations (see, e.g., Ref. [26]). However, the extreme compression occurs in the second stage, when a few-cycle soliton becomes actually a single-cycle soliton with an ultrabroad spectrum. We show that, in this stage, the process of further self-compression is strongly accelerated along with superbroad spectrum up-conversion, keeping the single-cycle soliton as a whole entity.

II. BASIC EQUATIONS AND FEW-CYCLE SOLITONS

For an adequate analysis of the extreme self-compression of laser pulses in a waveguide filled with a mixture of two gases with noticeably differing ionization potentials we should refer directly to the description of the self-action dynamics of the electromagnetic field in a medium within a wide spectral range based on the wave equation

$$\partial_{zz}^2 \mathcal{E} - \frac{1}{c^2}\partial_{tt}^2 \mathcal{E} = \frac{4\pi}{c^2}\partial_{tt}^2 \mathcal{P}, \tag{1}$$

where $\partial_{i=z,t}$ stands for the respective derivatives, c is the speed of light, and $\mathcal{P}(\mathcal{E})$ is the polarization response of the medium. In the case of a resonant interaction of the laser radiation with matter, when the signal frequency is close to the resonant transition frequency, the polarization response of the medium $\mathcal{P}$ can be defined based on a two-level-system model [6–8].

However, this model is inapplicable to the nonresonant case we consider here, when the carrier frequency is much less than the transition frequency. For the nonresonant interaction, contributions from other atomic levels should be considered. It is well known that generalizing to a three-level system leads to a change in the sign of the Kerr nonlinearity (from defocusing to focusing) [27]. The polarization response can be divided into two components $\mathcal{P} = \mathcal{P}_{\text{lin}} + \mathcal{P}_{nl}$. Here $\mathcal{P}_{\text{lin}} = \frac{1}{4\pi}[\int_{-\infty}^{t} \varepsilon(t - t')\mathcal{E}(t')dt' - \mathcal{E}]$ is responsible for the linear response of the medium, and $\mathcal{P}_{nl}$ describes the nonlinear part of polarization $\mathcal{P}$. Where ε is the linear dielectric permittivity in the system being considered, which in the optical domains can be written as

$$\varepsilon(\omega) = \varepsilon_o + a\omega^2 - \frac{\omega_D^2}{\omega^2}. \tag{2}$$

Note that the dielectric permittivity $\varepsilon(\omega)$ is determined by, in addition to the material dispersion of gases [28,29], the waveguide dispersion as well. Besides, for the case of interest the coefficient ω_D is defined mainly by the diameter of the waveguide.

In this case, the dispersion law for the wave $\mathcal{E} \sim \exp(i\omega\tau - i\kappa z)$, which propagates along z, has the form $\kappa = -\omega_D^2/\omega + a\omega^3$. One can control the role of the dispersion simply by changing the central frequency ω of the wide-band radiation. Specifically, for radiation having the frequency $\omega_b = (\omega_D^2/3a)^{1/4}$, the group-velocity dispersion parameter (GVD) $k_2 = \partial^2\kappa/\partial\omega^2$ becomes equal to zero. Correspondingly, for the wave fields having frequencies $\omega \gg \omega_b$, the field spectrum is concentrated in the region with normal group-velocity dispersion $k_2 > 0$, whereas for $\omega \ll \omega_b$ the dispersion is anomalous ($k_2 < 0$). Herein, we consider the case of anomalous dispersion, when $\omega \ll \omega_b$; therefore, the second term in Eq. (2) is small. Note that this situation can be implemented with sufficient ease by choosing the capillary diameter and gas pressure (see, e.g., Eq. [26]), since under typical conditions gas dispersion is low compared with waveguide dispersion.

The term $\mathcal{P}_{nl} = \mathcal{P}_1 + \mathcal{P}_2$ in Eq. (1) describes the nonlinear response of the mixture of gas with strongly different ionization potentials, e.g., helium and argon. A gas with a high ionization potential will ensure the Kerr-type inertia-free nonlinearity $\mathcal{P}_1 = \chi^{(3)}\mathcal{N}_a|\mathcal{E}|^2\mathcal{E}$, where $\chi^{(3)}$ is the atomic cubic nonlinear susceptibility (see, e.g., Refs. [30,31]), and $\mathcal{N}_a$ is the density of atoms with high ionization potential. The inertia-free nonlinearity is justified by virtue of the fact that the only physical mechanism which ensures the nonlinearity of the refraction index at short laser radiation duration and at such times is the nonlinearity of the polarization response of bound electrons. The characteristic time of the electron response delay is about the period of electron rotation around the nucleus. Allowing for the fact that helium has a high ionization potential (24 eV), this corresponds to a nonlinearity response duration of about 70 as, which is short compared with the durations considered in this work. To ensure nonstationarity of the nonlinearity, which will result in an increase in the carrier frequency of the laser pulse, we will use the mechanism of field ionization [32] of the second sort of gas with lower concentration. Correspondingly, the nonlinear response can be written as follows: $\partial_{tt}^2\mathcal{P}_2 = (\omega_p^2/4\pi)\mathcal{E}$. Here $\omega_{p,n}^2 = 4\pi e^2\mathcal{N}_{e,n}/m$, n_e is plasma density, n is the density of ionizing atoms ($n \ll \mathcal{N}_a$).

In the present paper we consider one-dimensional self-compression of a laser pulse in a waveguiding system. We assume that the spatial structure of the field is determined by the capillary mode. Structural modification of field distribution in the capillary under the action of Kerr and ionization nonlinearities was addressed in the papers [33,34]. The limitations were obtained on laser radiation power and plasma density at which the single-mode self-action persists. The corresponding conditions are fulfilled, for example, for a capillary 80 μm in diameter and a laser pulse with a duration of 25 fs and energy of several hundred microjoules.

To get an insight into the physics and propose a regular method of extreme soliton conversion, we first consider few-cycle solitons for which analytical treatment is necessary. To do so, we employ the well-proven slowly evolving wave approach (SEWA) [31] and use a one-way propagation wave equation, which is closed by the rate equation with the tunnel ionization as a main mechanism of plasma production [32]. Then the system of equations reads [5]

$$2c\frac{\partial^2 U}{\partial z\partial t} + \omega_D^2 U + \omega_p^2 U + \frac{\partial^2}{\partial t^2}(|U|^2 U) = 0, \tag{3a}$$

$$\frac{\partial \omega_p^2}{\partial t} = \left(\omega_n^2 - \omega_p^2\right)W(|U|). \tag{3b}$$

Here, $U = \mathcal{E}_x + i\mathcal{E}_y$, $\mathcal{E}_x$ and $\mathcal{E}_y$ are the corresponding components of the electric field in units of $(2\pi\chi^{(3)}\mathcal{N}_a)^{1/2}$, $t - z\sqrt{\varepsilon_o}/c \to t$ is the retarding time, and $W(|U|)$ is the tunnel ionization rate [32]. Note that Eqs. (3) describe the case of anomalous group-velocity dispersion and they are similar to the case of HC-PCFs considered in Ref. [26]. We only neglect the quantum absorptions connected with the atomic potential needed to ionize atoms, since Eqs. (3) comprise absorption corresponding to the fact that the newly born electrons acquire laser oscillation energy which in the tunnel regime for circular polarization exceeds the potential [19,35]. These energy losses can be minimized for linearly polarized light. However, we pay particular attention to the case of circularly polarized light for which soliton solutions can be found in explicit form and this greatly helps us to propose a way for extreme pulse compression.

In pure Kerr media ($\omega_p = 0$), there exists a class of few-cycle solitons [5]. In the dimensionless variables ($\tau = \omega_o t, \tilde{z} = \omega_D^2 cz/2\omega_o$, ω_o is the input carrier frequency), these solutions can be represented as follows:

$$U = \frac{\omega_D}{\omega_o}\gamma^{1/2}a(\xi)\exp\left[i(\tau + \gamma\tilde{z}) + i\phi(\xi)\right], \tag{4}$$

where $\xi = (\tau - \gamma\tilde{z})$, and γ^{-1} is the group velocity of the soliton in the (τ,$\tilde{z}$) plane. The soliton envelope $a(\xi)$ and nonlinear phase $\phi(\xi)$ obey the ordinary differential equations

$$a_\xi = \frac{\pm a}{(1 - 3a^2)}\left[\delta^2 - \frac{3}{2}(\delta^2 + 1)a^2 + \frac{(4 - 5a^2)a^2}{4(1 - a^2)^2}\right]^{1/2}, \tag{5a}$$

$$\phi_\xi = \frac{a^2(3 - 2a^2)}{2(1 - a^2)^2}, \tag{5b}$$

where $\delta^2 = \gamma^{-1} - 1$. One can see that Eqs. (5) are directly integrated and their solutions depend only on the parameter δ varying in the interval $0 \leqslant \delta^2 \leqslant 1/8$. It is useful to note that, in the limit $\delta \to 0$ corresponding to long pulses comprising many optical cycles, soliton solutions of the nonlinear Schrödinger equation have a sech form without phase modulation [30]:

$$a(\xi) = a_s = \frac{\sqrt{2}\delta}{\cosh(\delta\xi)}, \quad \phi \simeq 0. \tag{6}$$

For simplicity, we further refer to these solutions as the Schrödinger solitons. However, at higher δ, i.e., for few-cycle solitons, their envelope can still be described by sech-form with high accuracy (maximum deviation less than 3%) but with strong phase modulation given by Eq. (5b)

$$U(\xi) = \frac{\omega_D}{\omega_o}\sqrt{\gamma}a_s \exp\left[i\left(\tau + \gamma\tilde{z} + \int_{-\infty}^{\xi}\frac{a_s^2(3-2a_s^2)}{2(1-a_s^2)^2}d\xi\right)\right]. \tag{7}$$

This gives an ultrabroad spectrum which plays a very important role in ionization-induced pulse compression, especially taking into account that the highest frequencies of the spectrum are located in the central part of the pulse where ionization occurs. Next, we study the dynamics of soliton-like pulses in the ionization regime.

III. SOLITON SELF-COMPRESSION

We model pulse propagation in Eqs. (3) specifying initial distribution in the form of exact soliton solutions given by Eqs. (5). Figure 1 shows the dynamics of the pulse intensity $|\tilde{U}| = (\omega_o/\omega_D)|U|$ at $\beta \equiv \omega_n^2/\omega_D^2 = 0.01$ and $\delta = 0.1$ corresponding to the input soliton comprising four optical cycles. In what follows, the coordinate z is normalized to the dispersion length z_D, along which the pulse duration τ_p increases by $\sqrt{2}$ times in the linear case. One can see that the pulse is continuously shortening, reaching a minimum duration at the length $z = 55z_D$; at this point it has been compressed by 40 times, which corresponds to a duration of 250 as for the Ti:Sapphire laser ($\lambda = 0.8$ μm, 10 fs input pulse). It is important to note, as we see in Fig. 1, that in the process of shortening, the time structure of the envelope does not change, i.e., it corresponds to adiabatic decrease in the duration and increase in the carrier frequency. Thus, we conclude that, in this case, adiabatic soliton self-compression takes place up to the point $z = 55z_D$. Moreover, the soliton pulse reaching even single-cycle duration proceeds to compress by up-shifting the carrier frequency (to be more exact, by increasing the frequencies of the central part of the single-cycle soliton). To confirm our speculation that we deal with the soliton structure at each point, we performed an additional modeling: we chose the initial distribution as the field distribution formed at $z = 55z_D$ [see Fig. 1(a)] and modeled pulse propagation at $\beta = 0$ (i.e., ionization free). In this case, for such a field structure, the envelope distribution does not change in the process of propagation up to several hundreds of the compressed-pulse dispersion length ($z < 250z_D$). It is important to emphasize that, actually, the frequencies of the central part of the pulse lie in the violet range. Thus, the main question is how it happened. It should be also noted that we failed to get such extreme compression by using gas with one sort of atoms. This is easy to understand from the insets in Fig. 1: if, at the initial stage of propagation, the degree of ionization can be small (right inset) and the pulse compresses in the Schrödinger soliton manner, then due to the increase of the soliton amplitude full gas ionization occurs (left inset) which may cancel the Kerr nonlinearity and stop compression. This situation can be avoided by using a mixture of two gases with noticeably differing ionization potentials: gas with high potential (e.g., helium) provides the Kerr nonlinearity, and the other one with lower potential (e.g., argon) is ionized.

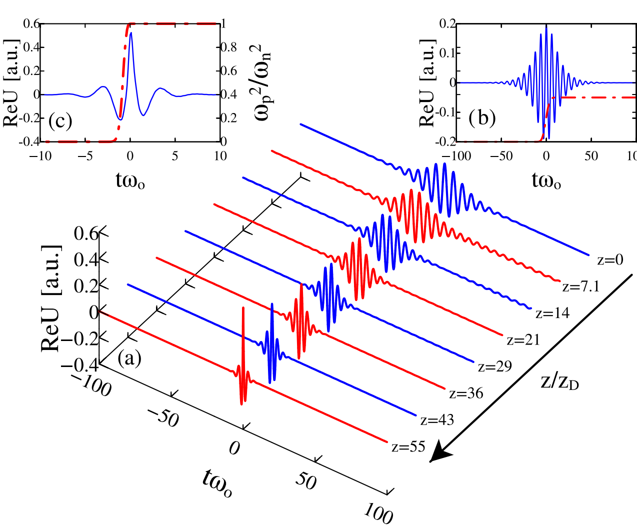

FIG. 1. (Color online) Dynamics of a laser pulse with initial profile given by Eqs. (5) at $\delta = 0.1$ and $\beta = 0.01$. Intensity of the pulse is normalized to the maximum value and z is in units of the linear dispersion length z_D. The insets show field distributions and ionization-degree profiles at $z = 0$ (right) and $z = 55z_D$ (left).

IV. SCHRÖDINGER SOLITON VS FEW-CYCLE SOLITON

For better understanding we first consider the difference of pulse compression between Schrödinger and few-cycle solitons.

Using the envelope approximation in the form $U(z,t) = \mathcal{A}(z,t)e^{i\varphi(z,t)}$ we substitute it into Eq. (3a) and subject $\omega = \varphi_t$, $\kappa = -\varphi_z$ to the linear dispersion equation

$$2c\omega\kappa + \omega_D^2 + \omega_p^2 = 0. \tag{8}$$

Then, by using the new retarding time $\tau = t - \frac{\omega_D^2}{2c}\int\frac{dz}{\omega^2(z)}$ and differentiating Eq. (8), for a slowly evolving envelope $\mathcal{A}(z,\tau)$, Eqs. (3) can be reduced to

$$2ic\left[\frac{\partial\mathcal{A}}{\partial z} + \frac{\omega_z}{2\omega}\mathcal{A}\right] + \frac{\omega_D^2}{\omega^3}\frac{\partial^2\mathcal{A}}{\partial\tau^2} + \omega|\mathcal{A}|^2\mathcal{A} = 0, \tag{9a}$$

$$\frac{\partial\omega^2}{\partial z} = \frac{1}{c}\frac{\partial\omega_p^2}{\partial\tau}, \tag{9b}$$

$$\frac{\partial\omega_p^2}{\partial\tau} = (\omega_n^2 - \omega_p^2)W(|\mathcal{A}|). \tag{9c}$$

Here we assumed that the group-velocity dispersion is mainly defined by the waveguide, i.e., $\omega_D \gg \omega_p$, and the gas dispersion is negligible. Note that, for amplitudes when the ionization is insignificant, Eq. (9a) is the nonlinear Schrödinger equation. It has a fundamental soliton solution:

$$|\mathcal{A}| = W_A \frac{\omega^2}{\omega_D} \frac{1}{\cosh\left(\frac{W_A \omega^4 \tau}{\omega_D^2}\right)}, \tag{10}$$

where $W_A = \int_{-\infty}^{\infty} |\mathcal{A}|^2 d\tau =$ const. is the soliton energy. For higher amplitudes when ionization comes into play, the carrier frequency ω is slowly up-shifting due to plasma production, in conformity with Eqs. (9b) and (9c). The system of equations (9) is self-consistent; the most important issues are (i) the frequency up-shift may be significant, depending on the propagation distance, and (ii) the second term describes the energy losses due to ionization. Although Eqs. (9) are still complex, they are quite transparent from the physical point of view, especially in respect to solitons. In particular, assuming that the solitonic structure of the wave packet is preserved, i.e., the carrier frequency slowly changes on the scale of soliton formation, we can present a soliton-like solution in the form

$$|\mathcal{A}| = \mathcal{A}_o \frac{\omega}{\omega_o} \frac{1}{\cosh\left(\frac{\mathcal{A}_o \omega^3 \tau}{\omega_D \omega_o}\right)}, \tag{11}$$

where $\mathcal{A}_o$ is the amplitude at the input. It is seen that the pulse-compression factor is $\tau_o/\tau_p = (\omega/\omega_o)^3$ (τ_o is the input pulse duration) increasing with frequency up-shifting over the propagation path. It is also important that, despite energy losses, the amplitude of the soliton-like pulse increases in proportion to the frequency. This results in an exponentially accelerating process of pulse compression, since the ionization rate $W(|\mathcal{A}|)$ is an exponentially growing function.

Then, we evaluate the law of variation of duration $\tau_p = \tau_o(\omega_o/\omega)^3$ of the quasisoliton solution (11) with respect to the evolution variable z for the case when the gas ionization degree is low, $\omega_n^2 \gg \omega_p^2$. To assess the medium length z_c over which the wave packet duration may turn to zero [$\tau_p(z_c) = 0$] we approximate the ionization probability $W(\mathcal{A})$ in power form:

$$W(|\mathcal{A}|) = \mu_m |\mathcal{A}|^{2m}, \quad m > 1. \tag{12}$$

In the case considered of circularly polarized radiation, the ionization rate does not depend on the field phase, even for pulses with a duration of several field oscillations [36]. Note that, in this case, laser-radiation dissipation typical of tunnel ionization is retained and described by the second term in equation (9a). Allowing for Eqs. (9b), (9c), and (12), we obtain the final solution for τ_p at $m > 1$:

$$\tau_p(z) = \tau_o \left[1 - z \frac{m\omega_n^2 \mu_m \alpha_m \mathcal{A}_o^{2m}}{2c}\right]^{\frac{3}{2m}}, \tag{13}$$

where

$$\alpha_m = \int_{-\infty}^{+\infty} \frac{dx}{\cosh^{2(m+1)} x}$$

is a number. One can see from Eq. (13) that the soliton duration will become equal to zero at the finite length z_c of the nonlinear medium:

$$z_c = \frac{2c}{m\omega_n^2 \mu_m \alpha_m \mathcal{A}_o^{2m}}. \tag{14}$$

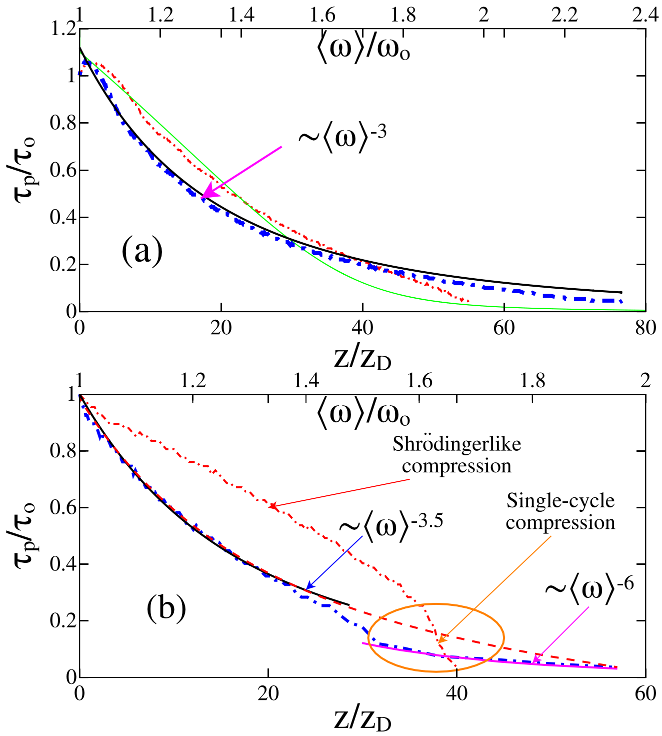

FIG. 2. (Color online) The dependence of pulse duration τ_p on the propagation distance (red dash-dotted line) and average frequency (blue dash-dotted line) for different δ: (a) $\delta = 0.1$ and (b) $\delta = 0.2$. Also, black and magenta curves are the corresponding approximations. The green solid curve in panel (a) is the same dependence $\tau_p(z)$ but calculated using Eqs. (9b) and (9c).

In what follows we compare the results of numerical simulation with the above-considered qualitative analysis.

Figure 2(a) presents the pulse duration τ_p as a function of z (red dash-dotted curve) together with the same dependence (green solid curve) but calculated for the soliton by using Eqs. (9b) and (9c). In this figure we also plotted by a blue dash-dotted curve the pulse duration as a function of average frequency (upper axis) and compared it with the dependence from Eq. (11) ($\tau_p \propto \omega^{-3}$). One can see that, when the pulse is long enough, the curves fit each other well, thus confirming the Schrödinger soliton compression stage. At this stage, the pulse is shortened by a factor of eight, whereas the frequency increases only twice. However, further along the propagation distance $z/z_D \sim 50$, when the pulse becomes actually a single-cycle pulse, the process of shortening is drastically accelerated but with slowly changing average frequency. As an illustration, we present in Fig. 2(b) the single-cycle soliton compression stage as a result of modeling for a soliton comprising two optical cycles ($\delta = 0.2$). The peculiarity of few-cycle solitons is that they are strongly phase modulated as follows from Eq. (5b) and this makes a strong impact on the process of the ionization-induced shortening.

Next, we evaluate the law of diminishing duration of the wave packet with respect to the carrier frequency for this case. Note that, as the wave packet spectrum width $\Delta\omega$ increases further in the process of shortening of the laser pulse duration or the initial duration of the wave packet, which is fed to the input of the nonlinear medium, Eq. (9a) will provide an incorrect description of the wave packet dynamics, since this equation is valid at $\Delta\omega/\omega \ll 1$. To ensure adequate qualitative description of the field in the wave packet for the case of $\Delta\omega/\omega \lesssim 1$, one should allow for an additional term, which is responsible for the dependence of the group velocity of the pulse on the field amplitude:

$$2ic\left[\frac{\partial \mathcal{A}}{\partial z}+\frac{\omega_z}{2\omega}\mathcal{A}\right]+\frac{\omega_D^2}{\omega^3}\frac{\partial^2\mathcal{A}}{\partial\tau^2}+\omega|\mathcal{A}|^2\mathcal{A}-2i|\mathcal{A}|^2\frac{\partial\mathcal{A}}{\partial\tau}=0. \tag{15}$$

In the framework of this equation, the soliton equation exists in the absence of ionization nonlinearity ($\omega_p = 0$) [37]. Let us use this solution to evaluate the variation in the wave packet duration in the case of smooth variation in the pulse carrier frequency in the process of gas ionization on the scales of the dispersion and nonlinear lengths. Allowing for the energy loss connected with gas ionization, we represent the solution of Eq. (15) in the following form:

$$\mathcal{A}=\frac{\mathcal{B}_s}{\sqrt{\omega}}\exp\left(i\phi+ihz\right), \tag{16a}$$

$$\frac{d\phi}{d\tau}=\frac{\omega^2}{2\omega_D^2}\mathcal{B}_s^2, \tag{16b}$$

$$\mathcal{B}_s^2=\frac{8hc}{1+\sqrt{1+4\kappa/\omega^2}\cosh(2\sqrt{\kappa}\tau)}, \tag{16c}$$

where $h=\frac{\mathcal{B}_m^2}{4c}(1+\frac{\mathcal{B}_m^2\omega}{2\omega_D^2})$, $\mathcal{B}_m$ is the maximum soliton amplitude, and $\kappa = 2c\omega^3 h/\omega_D^2$. This solution form allows for the decrease in the wave packet amplitude, which is due to the ionization loss. As follows from the formula for the phase [Eq. (16b)], a distinctive feature of the solution $\mathcal{A}$ by contrast with the nonlinear Schrödinger equation (NSE) solitons is a significantly strong frequency modulation in the laser pulse. Note that in terms of its structure, this frequency modulation [Eq. (16b)] is similar to the frequency modulation, which precise soliton solution (7) of the wave equation contains. One can see from Eq. (16c) that the duration of the soliton-like solution can be determined in terms of the dimensionless wave number κ. The decrease in the soliton duration is accompanied by a monotone increase in the carrier frequency ω and the maximum amplitude $\mathcal{B}_m$ of the wave packet. Therefore, we express κ in terms of the frequency and the value of the parameter $W_B=\int_{-\infty}^{+\infty}\mathcal{B}_s^2 d\tau$, which is retained in the process of self-compression of the wave packet:

$$\tau_p(\omega)=\frac{1}{\sqrt{\kappa}}\simeq\frac{1}{\omega\tan\left(\frac{W_B\omega^2}{4\omega_D^2}\right)}. \tag{17}$$

The black line in Fig. 2(b) represents the obtained dependence $\tau_p(\omega)$, which agrees well with the results of numerical simulation based on the system of equations (3), which one can see in the figure. Note that, in this frequency range, the soliton duration (17) can be approximated by the law $\tau_p \propto \omega^{-3.5}$. In fact, due to the rapid dependence of the ionization rate on the field intensity, the gas is essentially ionized within the hump of the pulse where the highest frequencies of the few-cycle soliton spectrum are located. This obviously enables efficient extreme compression of the central part of the pulse by slowly increasing the average frequency. This means that the ionization losses are less essential compared with the case of Fig. 2(b) at $z/z_D \lesssim 35$. This stems from the fact that, due to higher amplitudes, for few-cycle solitons ionization occurs only in a small central part, even when reaching full ionization degree as seen in Fig. 1(a), thus less affecting the other larger part of the soliton. This effect is more pronounced on a second short stage of extreme compression at $z/z_D \sim 36$ to 40 where an actual single-cycle soliton further shortens by increasing frequencies in a narrow central part only, as is seen in the left inset of Fig. 1. At this stage, an average frequency should vary slowly, as we see in the frequency dependence of the pulse duration in Fig. 2(b): $\tau_p \propto \omega^{-6}$.

V. OPTIMIZATION OF PULSE SHORTENING

To avoid complex high-order soliton dynamics [25] and thus to get the highest compression efficiency, the soliton order should be less than two. We have scanned the high-order soliton parameter $\mathcal{N}$ and present in Figs. 3(a) and 3(b) the characteristic dependence of the pulse duration on z at different $\mathcal{N} = 1$, 1.2, 1.3, and 1.4 for $\beta = 0.01$ and 0.04. It is seen from the figures that, with increasing β and $\mathcal{N}$, the rate of the the laser-pulse shortening increases. At $\mathcal{N} \leqslant 1.4$, soliton formation is observed in the process of insignificant radiation into the continuous spectrum. Consequently, the duration of

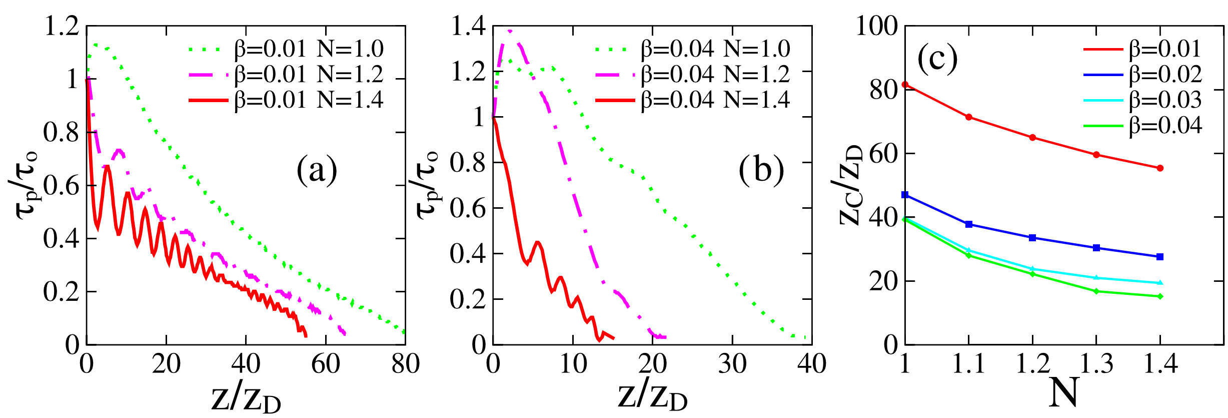

FIG. 3. (Color online) (a), (b) Pulse duration as a function of z for different values of $\mathcal{N}$ and two different β: (a) $\beta = 0.01$ and (b) $\beta = 0.04$. (c) Dependence of pulse-compression length on $\mathcal{N}$ and β.

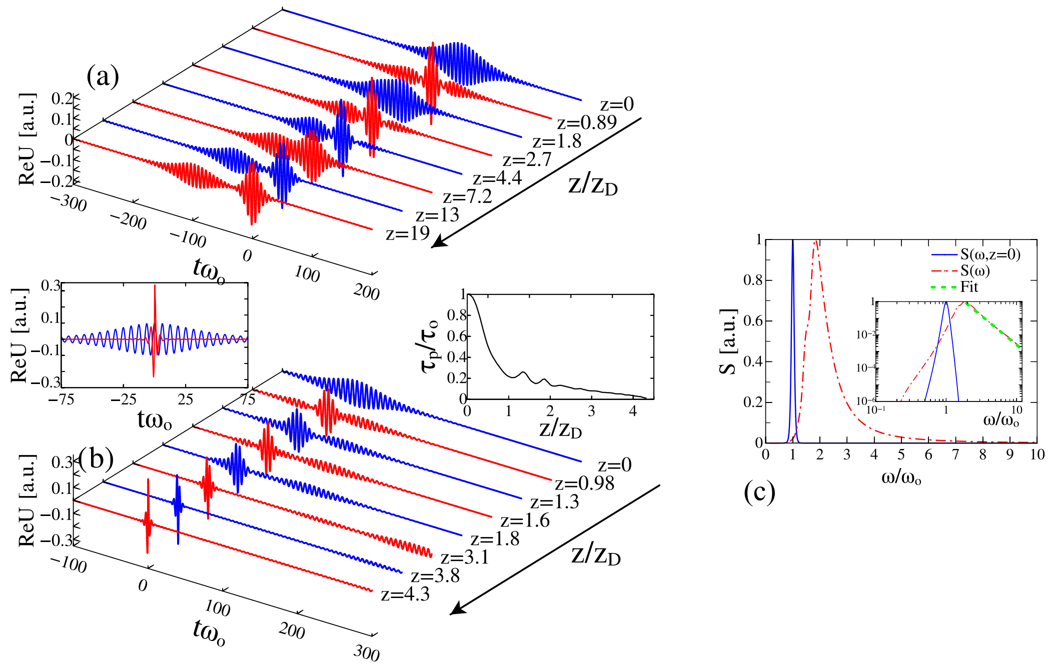

FIG. 4. (Color online) Dynamics of laser pulse at $\delta = 0.03$, $\mathcal{N} = 2.1$ for two cases: (a) for $\beta = 0$ (no ionization) and (b) $\beta = 0.02$. The left-hand inset in panel (b) shows pulse distributions at $z = 0$ (blue line) and $z = 4.3z_{\text{diss}}$ (red line). The right-hand inset in panel (b) shows the dependence of the normalized pulse duration of the wave τ_p/τ_o on z ($z_D = 360$). (c) Distributions of the power spectrum for the input and compressed pulses at $\mathcal{N} = 2.1$, $\delta = 0.03$, and $\beta = 0.02$. The blue curve corresponds to the initial spectrum, and the red dashed curve to the spectrum of the compressed pulse. The inset shows the spectra on logarithmic axes. The green lines show the approximation of the right-hand spectrum of the compressed pulse using the power law $S(\omega) \propto 1/\omega^{3.5}$.

the soliton decreases monotonically [see Figs. 3(a) and 3(b)]. However, at $\mathcal{N} \sim 1.4$, oscillations appear depending on the pulse duration $\tau_p(z)$. In Fig. 3(c) we presented the dependence on the parameters β and $\mathcal{N}$ of the compression length z_C at which the duration of the wave packet is compressed to 250 as. It is seen that by choosing the parameters β and $\mathcal{N}$ one can decrease the compression length z_C significantly. For example, if one specifies a pulse with the parameters $\delta = 0.1$ and $\mathcal{N} = 1$ at $\beta = 0.01$ at the input to the medium, then the compression length is $z_C = 83z_D$. For a pulse with the parameters $\delta = 0.1$ and $\mathcal{N} = 1.4$ at $\beta = 0.04$, the compression length decreases by a factor of 5.5 ($z_C = 15z_D$).

Note that, for longer pulses, the compression length increases considerably. In this case, we can use initial conditions as $U(\tau) = \sqrt{2}\mathcal{N}\delta\exp(i\tau)/\cosh(\delta\tau)$, which in the absence of ionization ($\beta = 0$) disintegrates into a sequence of solitons with parameters $\delta_n = (2n-1)\delta$, where $n = 1,\dots,[\mathcal{N}]$ is a sequence of integers [5]. Figure 4(a) presents the results of numerical modeling for $\delta = 0.03$ and $\mathcal{N} = 2.1$. We see that, at $z = 0.89z_{\text{diss}}$, the pulse is compressed with the highest efficiency, and then it splits into two solitons with $\delta_1 = 0.03$ and $\delta_2 = 0.09$. Thus, the duration of the second soliton is three times as short as that of the initial distribution. Note that the second soliton lags behind the first one, as the soliton velocity γ decreases with increasing δ. We can expect higher efficiency of pulse compression in the ionization regime. Figure 4(b) shows the dynamics of a pulse with the same parameters, but with the ionization allowed for, as for $\beta = 0.02$. At the initial stage ($z < z_D$), when the ionization is absent (due to the smallness of the amplitude in the pulse), the dynamics of the laser field is close to the case of $\beta = 0$. As a result of the splitting of the initial distribution, the high-intensity soliton (4) is excited, which starts ionizing the gas additionally. As a result, the intensive pulse starts compressing fast and outstrips the second pulse, since the group velocity of the wave packet grows with increasing carrier frequency. The left-hand inset in Fig. 4(b) shows pulse distributions at $z = 0$ and $z = 4.3z_D$, and the right-hand inset shows the dependence of the normalized duration τ_p of the wave packet on z, wherefrom it is seen that the pulse is compressed by 100 times. In dimensional units, the initial duration corresponds to 25 fs, and the duration of the compressed pulse is equal to 250 as. The compressed pulse contains 50% of the initial energy.

Figure 4(c) shows the normalized distributions of the power spectra

$$\left| S(\omega) = \int_{-\infty}^{+\infty} \text{Re}[U(\tau)]e^{i\omega\tau}d\tau \right|^2$$

for the initial and compressed wave packets (the blue and red dashed curves, respectively). It follows from this figure that the spectrum of the output pulse becomes significantly wider and drops smoothly towards the short-wave region. Specifically, the average carrier frequency increases by 2.5 times ($\langle\omega_{\text{out}}\rangle \simeq 2.5\langle\omega_{\text{in}}\rangle$), and the average spectrum width increases by 60 times ($\langle\Delta\omega_{\text{out}}\rangle \simeq 60\langle\Delta\omega_{\text{in}}\rangle$). For finding the law of spectrum drop, we plot the spectra on logarithmic axes. The green dots show the approximation of the compressed-pulse spectrum. The analysis shows that the short-wave part of the compressed-pulse spectrum is described well by the law $S_{\text{Fit}} \propto 1/\omega^{3.5}$. The power-law behavior of the spectrum is connected with the fact that effective energy transfer occurs from the main part of the pulse to the short-wave part of the spectrum, as there is almost no dispersion at high frequencies. This is an indication that the formed field discontinuity is somewhat weaker compared than that caused by a shock wave.

An additional investigation of the influence of the small asymmetry of the soliton-type profile upon shortening the laser-pulse duration was performed. The results of the numerical simulations for the initial distributions,

$$U(\tau) = \frac{\sqrt{2}\mathcal{N}\delta(1+\alpha\tau)\exp(i\tau)}{\cosh(\delta\tau)}, \tag{18}$$

with different parameters $\alpha = 10^{-2},\ldots,10^{-1}$ ($\mathcal{N} = 2.1$, $\delta = 0.03$) demonstrate that the self-compression regime is stable. The self-compression length increases only slightly due to transformation of the initial distribution to the soliton one.

VI. CONCLUSION

In conclusion, we have proposed and studied a method of extreme pulse compression when the Kerr and ionization nonlinearities are independently controlled by using a mixture of gases with significantly different ionization potentials. In this case, the system dispersion is controlled entirely by varying the waveguide diameter because, under the usual conditions, the gas dispersion is low compared with the dispersion of the waveguide system. This allows the generation of single-cycle pulses in the visible and ultraviolet domain. To perform qualitative analysis of self-compression of soliton-like laser pulses, we obtained a simplified system of equations, which allows us to study the dynamics of the wave packet in the case when the carrier frequency of the laser pulse can vary significantly in the process of ionization of the gas with a lower ionization potential. The field evolution is described by a self-consistent system of two equations: (i) the equation for the slow field envelope, and (ii) the equation of spatiotemporal geometric optics, which describes the variation in the spectral composition of the laser pulse in the process of gas ionization. It is shown in the framework of this approximate system of equations that the duration of the wave packet becomes equal to zero at the finite length of the nonlinear medium. The duration of the NSE solitons is shown to decrease with an increase in the carrier frequency in the process of gas ionization obeying the law $\tau_p \propto \omega^{-3}$, whereas for solitons of the derivative nonlinear Schrödinger equation, the duration decreases obeying the law $\tau_p \propto \omega^{-3.5}$. Good agreement of the results of numerical simulation with the qualitative analysis is demonstrated.

Finally, we present estimates for experimental realization. For a 25 fs, 0.2 mJ laser pulse (wavelength $\lambda = 0.8$ μm) propagating in a capillary of 40 μm in diameter filled with He under a pressure of 1 bar and Ar at a pressure of 2 torr, the numerical simulations show that the pulse can be compressed down to 250 as with pulse energy of 0.1 mJ. To obtain higher-energy pulses, it is reasonable to consider laser pulses at a wavelength of $\lambda = 4$ μm. Similar estimates for the same value of the dispersion can be obtained by considering a capillary with a wider diameter. If one employs a capillary with a diameter of 90 μm, one can compress a 90 fs pulse with an energy of 3.6 mJ down to a 0.9 fs, 1.8 mJ pulse.

ACKNOWLEDGMENTS

This paper was partially supported by the RFBR (Projects No. 13-02-00755, No. 14-02-01180, No. 15-32-20641, and No. 14-22-02076) and by the Ministry of Education and Science (Agreement No. 02.B.49.21.0003).

[1] A. Nazarkin and G. Korn, Phys. Rev. Lett. **83**, 4748 (1999).
[2] A. V. Husakou and J. Herrmann, Phys. Rev. Lett. **87**, 203901 (2001).
[3] J. M. Dudley, G. Genty, and S. Coen, Rev. Mod. Phys. **78**, 1135 (2006).
[4] A. Sakovich and S. Sakovich, J. Phys. A: Math. Gen. **39**, L361 (2006).
[5] S. A. Skobelev, D. V. Kartashov, and A. V. Kim, Phys. Rev. Lett. **99**, 203902 (2007).
[6] R. K. Bullough and F. Ahmad, Phys. Rev. Lett. **27**, 330 (1971); J. C. Eilbeck *et al.*, J. Phys. A **6**, 1337 (1973).
[7] E. M. Belenov, P. G. Kryukov, A. V. Nazarkin, A. N. Oraevskii, and A. V. Uskov, JETP Lett. **47**, 523 (1988).
[8] A. E. Kaplan and P. L. Shkolnikov, Phys. Rev. Lett. **75**, 2316 (1995).
[9] A. E. Kaplan, Phys. Rev. Lett. **73**, 1243 (1994).
[10] D. F. Gordon, B. Hafizi, R. F. Hubbard, J. R. Peñano, P. Sprangle, and A. Ting, Phys. Rev. Lett. **90**, 215001 (2003).
[11] O. Shorokhov, A. Pukhov, and I. Kostyukov, Phys. Rev. Lett. **91**, 265002 (2003).
[12] G. A. Mourou, T. Tajima, and S. V. Bulanov, Rev. Mod. Phys. **78**, 309 (2006).
[13] M. Lontano *et al.*, Phys. Scr. **63**, 141 (1996).
[14] T. M. Antonsen, Jr. and Z. Bian, Phys. Rev. Lett. **82**, 3617 (1999).
[15] E. Yablonovich, Phys. Rev. A **10**, 1888 (1974).
[16] W. M. Wood, G. B. Foght, and M. C. Downer, Opt. Lett. **13**, 984 (1988); W. M. Wood, C. W. Siders, and M. C. Downer, Phys. Rev. Lett. **67**, 3523 (1991).
[17] F. Brunel, J. Opt. Soc. Am. B **7**, 521 (1990).
[18] J. Dai, X. Xie, and X.-C. Zhang, Phys. Rev. Lett. **97**, 103903 (2006).
[19] V. B. Gildenburg *et al.*, IEEE Trans. Plasma Sci. **21**, 34 (1993).
[20] A. V. Kim *et al.*, Phys. Rev. A **42**, 2493(R) (1990).
[21] S. A. Skobelev, A. V. Kim, and O. Willi, Phys. Rev. Lett. **108**, 123904 (2012).
[22] P. St. J. Russell, Science **299**, 358 (2003).
[23] A. B. Fedotov, E. E. Serebryannikov, and A. M. Zheltikov, Phys. Rev. A **76**, 053811 (2007).
[24] P. Hölzer, W. Chang, J. C. Travers, A. Nazarkin, J. Nold, N. Y. Joly, M. F. Saleh, F. Biancalana, and P. St. J. Russell, Phys. Rev. Lett. **107**, 203901 (2011).
[25] M. F. Saleh, W. Chang, P. Hölzer, A. Nazarkin, J. C. Travers, N. Y. Joly, P. St. J. Russell, and F. Biancalana, Phys. Rev. Lett. **107**, 203902 (2011).
[26] W. Chang, P. Hölzer, J. C. Travers, and P. St. J. Russell, Opt. Lett. **38**, 2984 (2013).

[27] N. B. Delone and V. P. Krainov, *Fundamentals of Nonlinear Optics of Atomic Gases* (Wiley, New York, 1988).
[28] M. Born and E. Wolf, *Principles of Optics* (Pergamon, New York, 1968).
[29] A. Dalgarno and A. E. Kingston, Proc. R. Soc. London, Ser. A **259**, 424 (1960).
[30] G. P. Agrawal, *Nonlinear Fiber Optics* (Academic Press, San Diego, 2001).
[31] T. Brabec and F. Krausz, Rev. Mod. Phys. **72**, 545 (2000).
[32] V. S. Popov, Usp. Fiz. Nauk **174**, 921 (2004).
[33] G. Tempea and T. Brabec, Opt. Lett. **23**, 762 (1998).
[34] G. Tempea and T. Brabec, Opt. Lett. **23**, 1286 (1998).
[35] P. B. Corkum, N. H. Burnett, and F. Brunel, Phys. Rev. Lett. **62**, 1259 (1989).
[36] G. L. Yudin and M. Yu. Ivanov, Phys. Rev. A **64**, 013409 (2001).
[37] K. Porsezian and K. Nakkeeran, Phys. Rev. Lett. **76**, 3955 (1996).